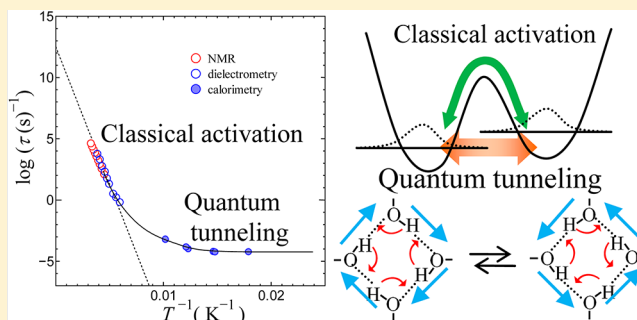


## Quantum Tunneling in the Quadruple Proton Rearrangement on a Hydroxyl Hydrogen Bond Ring in Calix[4]arene

Kouhei Ueda<sup>\*,†</sup> and Masaharu Oguni

Department of Chemistry, Graduate School of Science and Engineering, Tokyo Institute of Technology, 2-12-1 O-okayama, Meguro-ku, Tokyo 152-8551, Japan

**ABSTRACT:** Proton rearrangement rates in hydrogen bond networks are dominated by classical activation and quantum tunneling at higher and lower temperatures, respectively. Calix[4]arene (C4A) has a square-ring network composed of four hydroxyl groups with the O...O length of ~0.265 nm. Calorimetry and dielectric relaxation measurements were applied to determination of the rates in the crystals of C4A and its deuterium analogue (C4A-d). The rearrangement rates in C4A-d exhibited Arrhenius dependence in the measured temperature range. On the other hand, the rates in C4A showed the same dependence as those in C4A-d above 200 K, deviated from this dependence at around 180 K, and became independent of temperature at around  $10^{-4}$  s<sup>-1</sup> below 100 K. This evidenced that the tunneling in the quadruple proton rearrangement proceeds at a very slow rate of  $10^{-4}$  s<sup>-1</sup>. This is the first determination by calorimetry of the proton tunneling rate.



## 1. INTRODUCTION

The positional and orientational states of atomic nuclei and the dynamical properties associated with the change between the states are ordinarily described well by a picture recognizing the nuclei as classical particles. In cases where protons are rearranged in hydrogen bonds, the classical process takes place with surmounting of a potential barrier. Provided that two states of **1** and **2** are allowed for the configurations of protons, the rate  $\tau^{-1}$  for the rearrangement between the two states is given by a relation of  $\tau^{-1} = k_{12} + k_{21} = (K + 1)k_{21}$ , where  $k_{12}$  and  $k_{21}$  represent kinetic constants from the state **1** to **2** and from the state **2** to **1**, respectively, and  $K = k_{12}/k_{21}$  is the equilibrium constant. Let the **1** and **2** be the ground and excited states, respectively; namely, assume that the energy of state **2** is higher than that of **1**. At lower temperatures, the population of the state **2** in equilibrium becomes negligible, and the  $\tau^{-1}$  approaches  $k_{21}$ . At higher temperatures, because the populations of the two states become equal, the values of  $k_{12}$  and  $k_{21}$  become equal as well, and the  $\tau^{-1}$  approaches  $2k_{21}$ . In view that the  $\tau^{-1}$  changes gradually between  $k_{21}$  and  $2k_{21}$  over a wide temperature range while the value of  $k_{21}$  itself changes by many orders of magnitude, the factor of 2 is rather small, and the  $\tau^{-1}$  experimentally determined apparently obeys an Arrhenius equation in many crystalline systems.<sup>1–6</sup>

$$\tau^{-1} = \tau_0^{-1} \exp\left\{\frac{-\Delta\epsilon_a}{RT}\right\} \quad (1)$$

where  $\tau_0^{-1}$  is a pre-exponential factor and  $\Delta\epsilon_a$  is an activation energy for the rearrangement. In the cases where hydrogen bonds form a network, so-called ice rules are imposed on the arrangement of protons; each proton is unable to freely occupy

either of the two sites along the hydrogen bond, and simultaneous rearrangement of multiple protons is required. As the number of the simultaneously rearranged protons increases, the observance of the rules leads to the increase of the activation energy.<sup>1,2</sup> This classical rearrangement rate becomes small with decreasing temperature according to eq 1; it must be 0 at 0 K. However, the rearrangement of protons can proceed as well with penetration through the potential barrier because the proton is the lightest among atomic nuclei. Such a process is a quantum one called tunneling, and the rearrangement rate is independent of temperature in principle, except for a phonon-assisted effect; it is not 0 even at 0 K. Therefore, the tunneling mechanism becomes dominant in the rearrangement at lower temperatures.<sup>7–18</sup>

The proton tunneling dynamics in hydrogen bond networks has been studied most elaborately for benzoic acid (BA).<sup>7–10</sup> Two BA molecules form a dimer through two hydrogen bonds. Two protons are accessible only to two configurations under the ice rules. The rate of proton rearrangement, namely, transfer in this case, through the tunneling process has been studied by measuring the NMR spin–lattice relaxation time  $T_1$  as a function of temperature or magnetic field,<sup>7–10</sup> and the temperature dependence of the populations for the two configurations has been also examined by the neutron diffraction method.<sup>11</sup> The tunneling rate has been found below 50 K to be in the range of  $10^8$  s<sup>-1</sup>.<sup>7–10</sup>

Calix[4]arene (C4A) has an intramolecular hydrogen bond ring composed of four hydroxyl groups. Figure 1a–1 schemati-

Received: May 15, 2012

Revised: November 19, 2012

Published: November 21, 2012



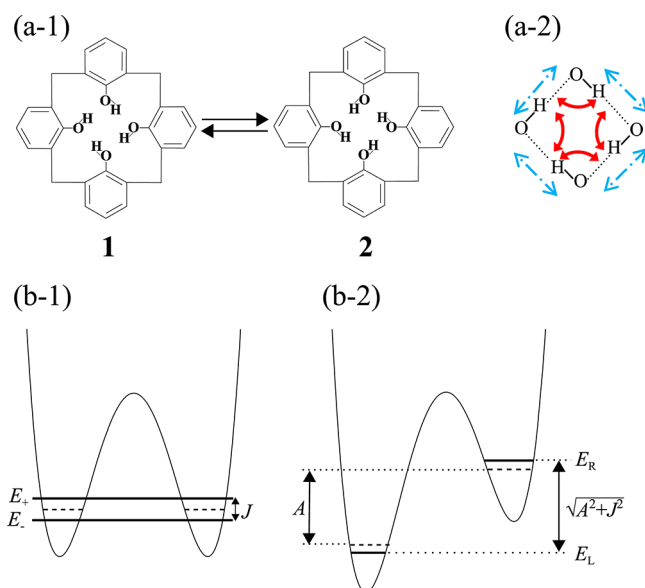


**Figure 1.** Two configurations, clockwise **1** and counterclockwise **2**, permitted under the classical ice rules for a quadruple proton within a C4A molecule (a-1), two possible pathways for the proton rearrangement (a-2), and a schematic drawing of symmetric (b-1) and asymmetric (b-2) potential curves concerning the two configurations and of energy levels of the associated ground states. Blue and red lines with arrows in (a-2) represent the rearrangement pathways through transfer of the protons on the O...O hydrogen bonds and through reorientation of the O–H bonds about the C–O axes, respectively. No other configurational disorder is present in the C4A molecule in the crystalline state.<sup>19</sup>

cally illustrates its molecular structure. According to the C4A crystal structure reported,<sup>19</sup> there exists a mirror symmetry plane perpendicular to the hydrogen bond ring plane. It is expected, as shown in the figure, that the hydroxyl protons are dynamically disordered between clockwise and counterclockwise configurations (tautomers **1** and **2**) through thermal activation at high temperatures and through tunneling at low temperatures. Here, it is noticed that two pathways are feasible for the proton rearrangement between the tautomers **1** and **2**, as represented by blue and red lines with arrows in Figure 1a-2. The protons in one way transfer along O...O hydrogen bonds with breaking of the respective OH chemical bonds like in BA,<sup>7–10</sup> and in the other way, they are rearranged by rotating the hydroxyl groups about the respective C–O axes, each with partial breaking of the hydrogen bond and re-formation of a new hydrogen bond with the other neighboring hydroxyl oxygen atom. This highly symmetric structure suggests that the two tautomers are considered to have equal or slightly different energies, as depicted by the potential curves in Figure 1b-1 and b-2, respectively. Provided that the energies of the tautomers are those in the case of Figure 1b-1, the ground states of the proton configurations split into two levels with an energy difference of  $J$  through penetration of the wave functions of the tautomers through the potential barrier. This is called a coherent proton tunneling. Should some asymmetric energy  $A$  be present between the potential energies of the two tautomers as in Figure 1b-2, on the other hand, the energy difference between the two ground states becomes a little larger than  $A$  due to the penetration effect of the wave functions; the splitting effect  $J$  due to the tunneling becomes smaller than that in the former case of Figure 1b-1. The quadruple proton configuration

is dynamically changing both in the classical and quantum pathways. The tunneling of this type is known as an incoherent one. The highly symmetric structure of C4A reported<sup>19</sup> indicates exactly or nearly  $A = 0$  at room temperature. Brougham et al. measured the NMR spin–lattice relaxation time  $T_1$  of *t*-butylcalix[4]arene (*t*-bC4A).<sup>12</sup> They found that the tunneling is observed in the range of 15–21 K with a rate of  $8 \times 10^7 \text{ s}^{-1}$ ; namely, the rate in *t*-bC4A is essentially the same as that in BA. They assigned the tunneling as attributed to the quadruple proton transfer in the ring of *t*-bC4A.<sup>12</sup> In view that tunneling phenomena potentially occur in methyl protons as well as hydroxyl protons in *t*-bC4A, however, their interpretation is of interest but not decisive.<sup>20,21</sup> In addition to this, Lang et al. observed, by NMR, the dynamics of quadruple proton rearrangement in a C4A molecule isolated in a nonpolar solvent.<sup>22</sup> The transfer rates were reported to be  $1.4 \times 10^2$ – $4.2 \times 10^4 \text{ s}^{-1}$  in the range of 221–304 K; they showed Arrhenius dependence with the activation energy of 36.8 kJ mol<sup>−1</sup>. The result is in clear contrast with the claim by Brougham et al. that the proton tunneling occurs at the rate of  $8 \times 10^7 \text{ s}^{-1}$ .<sup>12</sup>

In these situations, it is quite significant to explore the reality of the proton tunneling in the C4A molecule without methyl groups in the crystalline state. Adiabatic calorimetric and dielectric relaxation measurements were applied in the present study to the C4A (hereafter abbreviated C4A-*h*) and its deuterium-substituted (C4A-*d*) crystals. The former calorimetry detects enthalpy relaxation processes with characteristic times of  $10^6$ – $10^2 \text{ s}$ . The latter dielectrometry monitoring processes with characteristic times typically of  $10^2$ – $10^{-6} \text{ s}$  cover the time range between the calorimetry and the NMR method reported.<sup>12,22</sup>

Limbach et al. observed proton tunneling behavior in the rearrangement (transfer) of multiple protons on the NH...N-type hydrogen bond rings of pyrazole derivatives.<sup>13–18</sup> There, the two N atoms are the constituents of different pyrazole molecules, and the ring containing  $n$  hydrogen bonds is formed through connecting  $n$  molecules. It was indicated that when  $n = 2$  and 3, the protons are transferred in a concerted way and that when  $n = 4$ , a two-step process occurs involving a zwitterionic intermediate; thus, in the case of  $n = 4$ , the ice rules are violated in the transfer process, and ionic species mediate the whole proton transfer. The zwitterionic intermediate is considered to be stabilized by the effect of charge delocalization over the two relevant pyrazole molecular rings. Such a zwitterionic state potentially mediates the quadruple proton rearrangement in C4A, but it is unlikely that the mediation dominates the rearrangement; no dominance has been reported even in the cases of hydrogen bond rings composed of six hydroxyl groups such as in orthoboric acid<sup>1</sup> and Dianin's compound.<sup>2</sup>

## 2. SAMPLE PREPARATION AND MEASUREMENT METHODS

Ordinary C4A (C4A-*h*) was synthesized from *t*-bC4A-*h* according to the method reported.<sup>23</sup> The C4A-*h* crystal synthesized was purified twice by sublimation. Thus, the used sample was a powder. It is well-known that the C4A crystal possesses interspaces to allow solvent molecules to be included. The presence and absence of such included molecules were examined by dissolving the purified crystal into CDCl<sub>3</sub> and by measuring <sup>1</sup>H NMR of the solution. It was confirmed that no signal originating from other organic molecules than C4A-*h* was detected on the spectra, indicating that no solvent molecules

were included in the crystal. Deuteron-substituted crystal C4A-*d* was prepared by repeating, thrice, dissolution of the C4A-*h* into a CH<sub>2</sub>Cl<sub>2</sub> and CH<sub>3</sub>OD mixed solvent and removal of the solvent; only the hydroxyl protons within C4A were deuterated in this procedure. The prepared C4A-*d* was purified by sublimation, and the absence of the solvent molecules in the crystal was confirmed in the same way as that in the C4A-*h* crystal. The deuteron substitution ratio is expected to be more than 99%. The crystal structures of the prepared C4A-*h* and C4A-*d* were checked from their powder X-ray diffraction patterns and found to be identical to the reported one.<sup>19</sup>

Enthalpy relaxation measurements were carried out with an adiabatic calorimeter.<sup>24</sup> Dielectric relaxation measurements were performed with a homemade cryostat as well as a Solartron 1260 impedance analyzer and a Solartron 1296 signal buster. The sample pellets with a diameter of 10 mm and a thickness of 0.3–0.7 mm were prepared by pressing at 10 MPa under vacuum, sandwiched between two gold-coated copper plates as electrodes.

### 3. RESULTS AND DISCUSSION

Heat capacities and spontaneous enthalpy release or absorption rates were measured by intermittently heating the sample under adiabatic conditions, namely, repeating energy input and thermometry.<sup>24</sup> The enthalpy relaxation rates were derived from the spontaneous temperature drift rates ( $dT/dt$ ), observed in the thermometry periods, times the gross heat capacities of the calorimeter cell loaded with the sample. Figure 2a and b shows the temperature dependence of the relaxation

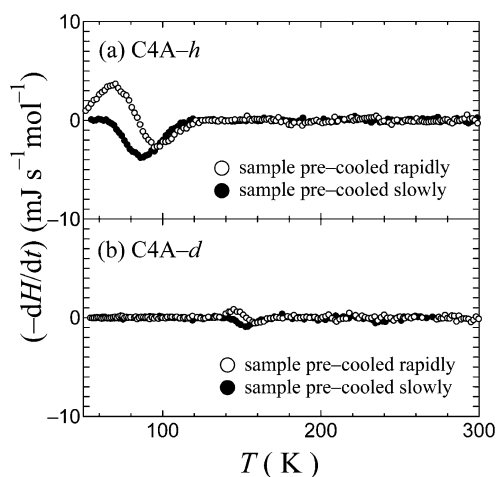


**Figure 2.** Temperature dependence of spontaneous enthalpy release or absorption rates, observed in the ordinary C4A (C4A-*h*) (a) and deuteron-substituted C4A (C4A-*d*) (b), upon intermittent heating.

rates observed for C4A-*h* and C4A-*d*, respectively. The measurements were executed for the two samples precooled at different speeds beforehand; one was cooled at a high speed of  $-10\text{ K min}^{-1}$  and the other at a low speed of  $-25\text{ mK min}^{-1}$ . The average heating speeds for the measurements were  $\sim 0.1\text{ K min}^{-1}$  in between the two, high and low, precooling speeds.

Figure 3a illustrates the enthalpic path, followed by the sample, associated with the temperature change for heat capacity measurements in a glass-transition region.<sup>1,24,25</sup> There, the enthalpy on the ordinate represents only the contribution from the configurational degree of freedom relevant to the freezing-in phenomenon; the contributions from all of the

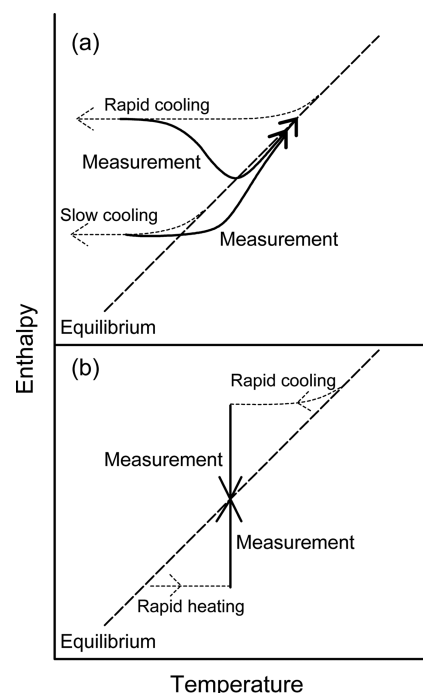


**Figure 3.** Enthalpic paths, followed by the sample, associated with the temperature change for heat capacity measurements (a) and for characterization of the relaxation function after a sudden jump of the sample's temperature (b) in a glass-transition range. Dashed lines in the both panels represent the equilibrium enthalpy curves concerning the proton-configurational degree of freedom. In the upper panel, when the sample is cooled rapidly or slowly as indicated by dotted lines with arrows, the enthalpy of the sample deviates from the dashed equilibrium line at higher or lower temperatures, respectively, due to lengthening of the equilibration time relative to the precooling speeds and is brought to the respectively different nonequilibrium states. The enthalpic states concerning all other degrees of freedom are reasonably assumed as in the respective equilibrium ones at any time.<sup>1,24–27</sup> In the lower panel, as indicated with dotted lines with arrows, the sample is cooled or heated rapidly toward the temperature at which the relaxation is followed and characterized, after having been aged at higher or lower temperatures, respectively, for a long time.<sup>28,29</sup>

other degrees of freedom are at the equilibrium values corresponding to each temperature at any time. The rapidly precooled sample is frozen, concerning the relevant configurational degree of freedom, in a relatively high-enthalpic state at low temperatures (as indicated with the upper dotted line with an arrow), and upon heating, it reveals a heat release effect in response to its return to the equilibrium state (as indicated with the upper solid line), which is probed by the calorimetry when the relaxation times for the relevant configurational degrees of freedom enter the calorimetric time scale range of  $10^6$ – $10^2$  s. On the other hand, the slowly precooled one is frozen in a relatively low-enthalpic state (see the lower dotted line with an arrow) and reveals a heat absorption effect upon the heating to attain its equilibrium state (see the lower solid line). In reality, the dependence in C4A-*d* (Figure 2b) is understood reasonably as attributed to a classical glass transition; the enthalpy relaxation appears only in a narrow temperature range of 20 K as usually found in the glass transitions in crystals where, in general, the relaxation times follow Arrhenius eq 1 with a single constant  $\Delta\epsilon_a$ .<sup>1,24–27</sup> However, the temperature dependence of the enthalpy relaxation rates in C4A-*h* (Figure 2a) is quite distinct in the character from that found in such typical glass

transitions.<sup>1,24–27</sup> The temperature range in which the enthalpy relaxation appeared is too wide; the range extends from below 50 up to 120 K. It is further noted that the isotope effect, namely, the difference between the C4A-*h* and C4A-*d*, regarding the midpoint of the temperature range in which the enthalpy relaxation phenomenon appeared, is too large, over 70 K. Considering that the deuterium-substitution isotope effect on the temperatures of the classical glass transitions is ordinarily 5 K or so,<sup>1,24–27</sup> the large value of 70 K should be recognized as reflecting that the process taking place in C4A-*h* is not simply a classical glass transition but a quantum tunneling.

On the basis of such a consideration, the rearrangement rate, which is equivalent to the inverse of the relaxation time  $\tau$ , was first estimated by following the enthalpy relaxation process for 50 ks after a sudden jump of the sample's temperature, as illustrated in Figure 3b,<sup>28,29</sup> and by fitting to the obtained relaxation curves the exponential function with a single  $\tau$ .

$$\Delta H(t) = \Delta H(0) \exp\left(-\frac{t}{\tau}\right) \quad (2)$$

Here, a pre-exponential factor  $\Delta H(0)$  is the difference in the enthalpy from the equilibrium state at the time  $t = 0$ , where the relaxation starts after the rapid heating or cooling, as illustrated in Figure 3b. Filled marks in the upper panel of Figure 4

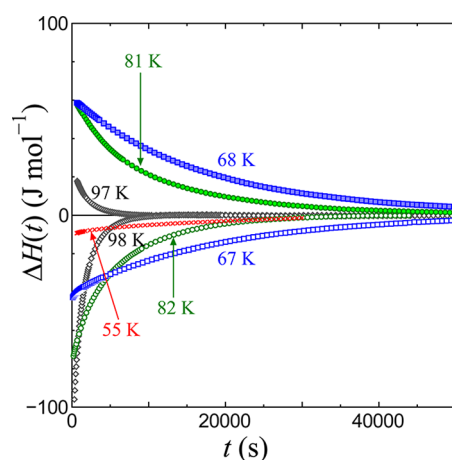


**Figure 4.** Enthalpy release or absorption processes due to proton tunneling in C4A-*h* at different temperatures. Filled marks in the upper panel represent the heat release processes observed after the samples were rapidly cooled to the written temperatures from 120 K. Open and cross marks in the lower panel represent the heat absorption processes observed after the samples were rapidly heated to the written temperatures from the 50 K to which the samples had been precooled slowly at  $-10 \text{ mK min}^{-1}$  from 120 K.

represent the obtained heat release processes observed after the samples were rapidly cooled to the written temperatures from 120 K, where they were aged for 15 min to attain their equilibrium states. Open and cross marks in the lower panel represent the heat absorption processes observed after the samples were rapidly heated to the written temperatures from

the 50 K to which the samples had been precooled slowly at  $-10 \text{ mK min}^{-1}$  from 120 K. The relaxation times, derived by fitting the exponential function (eq 2) to the data, are summarized in Table 1.

The proton rearrangement rate was determined second by measuring the dielectric loss as a function of temperature at some constant frequencies from 0.10 to 891 Hz. Figure 5 shows

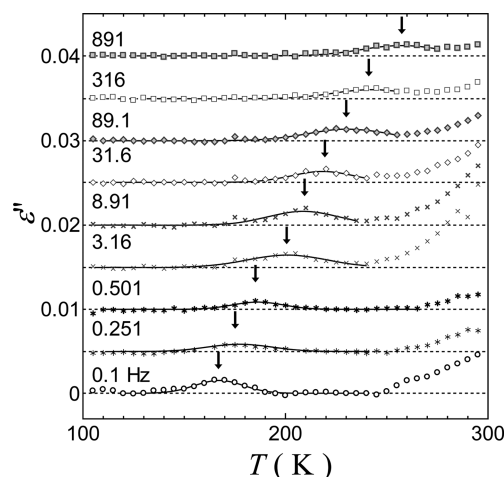


**Figure 5.** Dielectric loss peak displaying the rate of quadruple proton rearrangement in C4A-*h*. The origin of the ordinate  $\epsilon''$  was shifted upward by 0.005 in the order of increasing frequency  $f$ ; the  $f$  values are written inside of the figure.

the results with upward shifts in the ordinate by 0.005 in the order of increasing frequency. Loss peaks are, although small, definitely confirmed to be present, and their presence indicates that the proton rearrangement processes can be detected by the dielectric relaxation method. The peak temperatures were determined by fitting gauss functions to the data, as shown with solid lines in Figure 5. The peak temperatures decreased with decreasing operation frequency  $f$ , and the values derived are tabulated in Table 2. The rearrangement rate at a given peak temperature was evaluated by using a relation  $\tau^{-1} = 2\pi f$ , according to the Debye model, which has been used as reasonable in many systems.<sup>3–6,30</sup>

The rearrangement rates obtained by both methods are presented in Figure 6 on an Arrhenius plot, together with the literature data obtained by NMR by Lang et al.<sup>22</sup> The NMR data are in reasonable agreement with the present ones in their temperature dependence. The dependence at high temperatures above 200 K is well-fitted by the Arrhenius eq 1, as drawn with a blue dotted straight line for C4A-*h* and a red dashed straight line for C4A-*d*. The  $\tau_0^{-1}$  value as a pre-exponential factor is close to  $10^{13} \text{ s}^{-1}$ , reasonably corresponding to the frequency of molecular vibrations. The activation energy  $\Delta\epsilon_a$  was estimated to be 43  $\text{kJ mol}^{-1}$  for C4A-*h* and 47  $\text{kJ mol}^{-1}$  for C4A-*d* from the slopes of a blue dotted and a red dashed straight line, respectively.

**Table 1.** Characteristic times determined by enthalpy relaxation measurements

$T/\text{K}$	98 <sup>a</sup>	98 <sup>b</sup>	81 <sup>a</sup>	82 <sup>b</sup>	68 <sup>a</sup>	68 <sup>b</sup>	56 <sup>b</sup>
$\tau/\text{s}$	$1.7 \times 10^3$	$1.6 \times 10^3$	$9.9 \times 10^3$	$7.1 \times 10^3$	$1.7 \times 10^4$	$1.8 \times 10^4$	$1.7 \times 10^4$

<sup>a</sup>Samples were rapidly cooled to the written temperatures from 120 K, where they were aged for 15 min to attain their equilibrium states. <sup>b</sup>Samples were rapidly heated to the written temperatures from 50 K to which they had been precooled slowly at  $-10 \text{ mK min}^{-1}$  from 120 K.



Table 2. Temperatures Producing the Peak of Dielectric Loss at Constant Frequency

$f/\text{Hz}$	891	316	89.1	31.6	8.91	3.16	0.501	0.250	0.100
$T_{\text{peak,h}}/\text{K}$	257.3	242.6	230.9	218.3	208.8	200.9	186.4	177.4	167.3
$T_{\text{peak,d}}/\text{K}$	267.4	247.5	236.3	230.5	218.6				

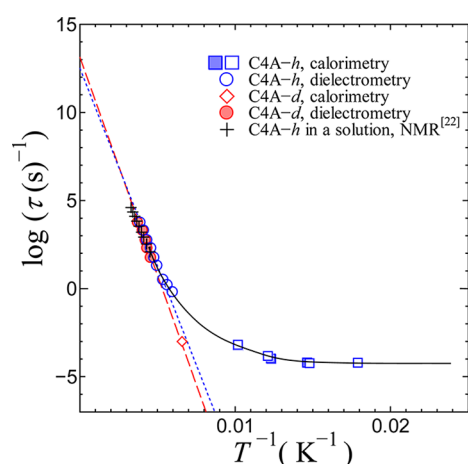


**Figure 6.** Temperature dependence of the proton/deuteron rearrangement rates for C4A-h and C4A-d on an Arrhenius plot. The former C4A-h reveals a low-temperature behavior of the rates asymptotic to  $10^{-4} \text{ s}^{-1}$ , indicating the progress of quantum tunneling. The solid, dashed, and dotted lines are guides for the eyes. Plus marks represent the literature data obtained by NMR.<sup>22</sup>

Deuteron substitution has been reported<sup>31,32</sup> to show, as a geometric isotope effect, a propensity to lengthen the O...O (N...N) distance and shorten the O–H (N–H) chemical bond length from a lot of structural data of strongly hydrogen bonded crystals. The  $\Delta\epsilon_a$  of the deuterated material is expected, based on this effect and a mass effect on the zero-point vibration, to differ from that of the ordinary, hydrated one. Actually, the  $\Delta\epsilon_a$  observed for deuterated BA is twice the value of ordinary BA in the high-temperature Arrhenius region. The transfer rates for the ordinary and deuterated BA are also much different even above 100 K. The similar large isotope effect has been also observed for other materials such as some pyrazole derivatives.<sup>13–18</sup> On the other hand, the  $\Delta\epsilon_a$  determined above for C4A-d is larger only by 10% than that for C4A-h, and the rearrangement rates for the two are almost the same in the classical region. Two reasons are raised as the potential for this relatively small isotope effect in C4A. One is that the geometric isotope effect is remarkably big in the hydrogen bonds with shorter O...O distances than a value of around 0.263 nm, while, on the other hand, it is very small in the bonds with the distances in a range of 0.264–0.285.<sup>31</sup> C4A and BA are situated near the border in their distances, 0.265 nm for C4A<sup>19</sup> and around 0.262 nm for BA<sup>33,34</sup> at room temperature. It is likely a potential that a large difference exists between the geometric isotope effects for C4A and BA. The other reason is that the hydrogen bond network in C4A is formed within a molecule while formed between molecules in BA and pyrazole derivatives. A possibility exists that the degree of the geometric isotope effect on the O...O distance in C4A is relatively small as compared with those in the cases of intermolecular hydrogen bonds.

As stated above, the rearrangement between the two tautomers **1** and **2** shown in Figure 1a-1 is feasible in two pathways; in one way, the rearrangement occurs through the transfer of four protons along the O...O hydrogen bonds like in

BA,<sup>7–10</sup> and in the other, it does by rotating each hydroxyl group about the C–O axis like that about B–O and C–O axes in orthoboric acid<sup>1</sup> and Dianin's compound,<sup>2</sup> respectively. In this respect, it is attractive to compare the  $\Delta\epsilon_a$  values per single hydrogen bond against the O...O lengths among some known crystals with hydrogen bond rings. In Dianin's compound crystal with hexagonal rings composed of six hydroxyl groups, the O...O length is 0.284 nm with a weak hydrogen bond, the rearrangement proceeds through reorientation of the hydroxyl group with breaking of the weak hydrogen bond, and the observed  $\Delta\epsilon_a$  per single bond is  $5.5 \text{ kJ mol}^{-1}$ .<sup>2</sup> In the orthoboric acid crystal with the similar hexagonal rings,<sup>35</sup> the length is 0.271 nm, with a little stronger hydrogen bond than that in the Dianin's compound, the rearrangement proceeds still through reorientation of the hydroxyl group, and the observed  $\Delta\epsilon_a$  per single bond is  $15 \text{ kJ mol}^{-1}$ .<sup>1</sup> In the present C4A crystal, the length is 0.265 nm, so that the hydrogen bond should be much stronger than that in the above two crystals. The  $\Delta\epsilon_a$  per single bond was evaluated to be  $\sim 11 \text{ kJ mol}^{-1}$  in reality. If the rearrangement proceeds through reorientation of the hydroxyl groups as well with complete breaking of the hydrogen bonds, the energy to break the bond must be bigger than the above two. The fact that the really observed activation energy is  $11 \text{ kJ mol}^{-1}$ , which is smaller than  $15 \text{ kJ mol}^{-1}$ , suggests the following two possibilities: One is that the rearrangement proceeds through transfer of protons along the O–H...O hydrogen bonds. This is consistent with that the value of  $11 \text{ kJ mol}^{-1}$  being close to the ones estimated for the proton transfer reaction in systems  $\text{H}_5\text{O}_2^+$  and  $\text{H}_3\text{O}_2^-$  with an O...O length of 0.265 nm.<sup>36</sup> The other possibility is that, on account of the reorientation angle being smaller in the C4A case than  $90^\circ$ , the hydrogen bond might not be completely broken even at the activated state upon reorientation of the hydroxyl group. There remains also a possibility that both processes occur at almost the same rates. The real situation cannot be determined at present, and its determination is fascinating and should be challenged in the future.

The most striking fact seen in Figure 6 is that the rates for C4A-h reveal Arrhenius dependence above 200 K, deviate from the dependence at around 180 K, and become independent of temperature below 100 K, approaching a constant value of around  $10^{-4} \text{ s}^{-1}$  at the lowest temperature; a solid line is a guide for the eyes. A quantum tunneling certainly dominates the proton rearrangement in the low-temperature regime, whereas a classical process dominates in the high-temperature one.

Here, it is significant to consider how the magnitude of the energy splitting  $J$  due to the tunneling is compared with the difference  $\Delta E$  between the real microscopic-state energies of quadruple proton configurations. For simplicity, we assume only two energy levels without degeneracy for each configuration. Then, the latter energy difference  $\Delta E$  can be assessed from the magnitudes of the enthalpies released or absorbed in their relaxation processes observed in Figure 4. The application of the exponential function (eq 2) to the enthalpy relaxation processes yields  $\Delta H(0)$  as the difference between the enthalpies at the two temperatures before and after the rapid

cooling/heating prior to the relaxation measurements. Because this  $\Delta H(0)$  value is given as functions of the energy difference  $\Delta E$  and the two temperatures, the  $\Delta E$  can be derived conversely from the  $\Delta H(0)$ . The  $\Delta E$  was assessed from the relaxation data to be  $(0.68 \pm 0.07)$  kJ mol<sup>-1</sup>. On the other hand, zero-level splitting  $J$  was estimated theoretically<sup>37</sup> to be  $2.2 \times 10^{-5}$  kJ mol<sup>-1</sup> for C4A in the gaseous phase, namely, for the quadruple proton configurations with an asymmetry energy of  $A = 0$ . The theoretically obtained  $J$  is too small in the order of magnitude as compared with the  $\Delta E$  assessed from the enthalpy relaxations; the real magnitude of  $J$  is expected to be further smaller than the theoretical value upon considering the presence of the large asymmetry energy  $A$ . This allows us to conclude that the potential energy curve for the quadruple proton configurations in C4A should be such as that drawn in Figure 1b-2 and therefore that the tunneling must be of an incoherent type assisted by phonons.

A potential way to experimentally ascertain the asymmetric feature of the double well potential is to follow the proton populations as a function of temperature. In the case with  $A = 0$ , the populations should be kept the same between the two potential minimum sites down to 0 K, as found in an isolated hydrogen bond system of 5-bromo-9-hydroxyphenalenone.<sup>38,39</sup> Meanwhile, in the case with  $A \neq 0$ , significantly, it should change with decreasing temperature. So far, for the C4A crystal structure, space group  $P6_3/m$  that has mirror symmetry perpendicular to the plane of hydrogen bond ring has been reported,<sup>19</sup> indicating that the situation with  $A = 0$  is realized at room temperature. However, the space group was determined based on the data of the powder sample because the guest-free C4A sample is available only in the powdery state. Unfortunately, space group  $P6_3$  follows the same rule for the forbidden diffraction peaks as  $P6_3/m$ . It is difficult in fact to decide, from the structural data, whether the space group should be assigned as  $P6_3/m$  or  $P6_3$ . In order to get clear evidence for the decision of the space group or the proton populations as a function of temperature, it is necessary to execute a structural study by using a single crystal. If the guest-inclusion C4A crystal reveals the same proton tunneling as guest-free C4A, it will be preferable to use such guest-molecule inclusion compounds. A calorimetric study to examine if the same tunneling occurs in the inclusion compounds is now under progress in our laboratory.

In passing, Bove et al.<sup>40</sup> reported, based on the measurements of incoherent quasielastic neutron scattering, that the proton tunneling in ice occurs at  $2.7 \times 10^{11}$  s<sup>-1</sup> and proposed that the tunneling is connected to a concerted transfer of six protons in the hexagonal ring composed of six hydroxyl groups. In view of the present results, the tunneling rate for the simultaneous transfer of six protons is understood as being too small to be observed even for the systems with an O...O length of 0.265 nm. In reality, the O...O length in ice is around 0.275 nm, in between the cases of Dianin's compound and orthoboric acid with O...O lengths of 0.284 and 0.271 nm, respectively.<sup>2,35</sup> In such situations, the rearrangement of protons would be preferably brought through reorientation of the hydroxyl groups while breaking the hydrogen bonds. Using the parameters for the Arrhenius equation obtained in Dianin's compound,<sup>2</sup> a classical glass transition is expected to take place at 111 K as the temperature at which the rate becomes  $10^{-3}$  s<sup>-1</sup>. The freezing-in phenomenon observed at around 111 K of the occupancy ratio between the two permitted proton configurations is also well explained by the presence of the glass

transition.<sup>2</sup> The orthoboric acid crystal is known to reveal a classical glass transition at 290 K.<sup>1</sup> If the tunneling rate for the rearrangement were on the order of  $10^{11}$  s<sup>-1</sup>, aside from whichever of the two rearrangement processes makes progress, no classical Arrhenius behaviors of rearrangement rates nor classical glass transitions should be realized in these crystals. Thus, the proposition by Bove et al.<sup>40</sup> for the proton transfer in ice is difficult to accept consistently with the results of the present C4A and previous crystals.<sup>1,2</sup>

#### 4. CONCLUSIONS AND PERSPECTIVE

Two things should be pointed out in connection with the finding of proton tunneling in the present work. One is that the quantum tunneling in the quadruple proton rearrangement of C4A proceeds at a very slow rate differently from that reported before.<sup>12</sup> The finding elucidates the importance of calorimetry in the characterization of quantum tunneling; this is really the first report to have analyzed quantum tunneling rates by the method. The other is that because the quantum states of the four protons are represented as the wave functions coupled between the orbital and nuclear spins of the protons, the rearrangement rates should be affected strongly by the magnetic fluctuation generated by electron spins. It is desired to study in the future how the enthalpy relaxation rate in C4A is affected by the fluctuation of the magnetic field. In addition, considering that some kind of tunneling phenomenon has been observed in *t*-bC4A,<sup>12</sup> the substituent effects on the tunneling phenomenon presently found in C4A should be examined in the future as well.

#### AUTHOR INFORMATION

##### Corresponding Author

\*Fax: +81-48-462-4661. Tel: +81-48-462-9410. E-mail: ueda.kohei@riken.jp.

##### Present Address

<sup>†</sup>RIKEN, 2-1 Hirosawa, Wako-shi, Saitama 351-0198, Japan.

##### Notes

The authors declare no competing financial interest.

#### REFERENCES

- (1) Oguni, M.; Matsuo, T.; Suga, H.; Seki, S. *Bull. Chem. Soc. Jpn.* **1977**, *50*, 825–833.
- (2) Bernhard, T.; Zimmermann, H.; Haebleren, U. *J. Chem. Phys.* **1990**, *92*, 2178–2186.
- (3) Moriya, K.; Matsuo, T.; Suga, H. *J. Phys. Chem. Solids* **1983**, *44*, 1103–1119.
- (4) Park, J.-H. *Phys. Rev. B* **2004**, *69*, 054104/1–054104/6.
- (5) Chen, R. H.; Chang, R. Y.; Shern, S. C. *J. Phys. Chem. Solids* **2002**, *63*, 2069–2077.
- (6) Chen, R. H.; Shem, C.-C.; Fukami, T. *J. App. Phys.* **2005**, *98*, 044104/1–044104/7.
- (7) Brougham, D. F.; Horsewill, A. J.; Jenkinson, R. I. *Chem. Phys. Lett.* **1997**, *272*, 69–74.
- (8) Heuer, A.; Haebleren, U. *J. Chem. Phys.* **1991**, *95*, 4201–4214.
- (9) Jenkinson, R. I.; Ikram, A.; Horsewill, A. J.; Trommsdorff, H. P. *Chem. Phys.* **2003**, *294*, 95–104.
- (10) Xue, Q.; Horsewill, A. J.; Johnson, M. R.; Trommsdorff, H. P. *J. Chem. Phys.* **2004**, *120*, 11107–11119.
- (11) Wilson, C. C.; Shankland, N.; Florence, A. J. *Chem. Phys. Lett.* **1996**, *253*, 103–107.
- (12) Brougham, F. B.; Caciuffo, R.; Horsewill, A. J. *Nature* **1999**, *397*, 241–243.
- (13) Limbach, H.-H.; Schowen, K. B.; Schowen, R. L. *Phys. Org. Chem.* **2010**, *23*, 586–605.

- (14) Lopez, J. M.; Langer, U.; Torres, V.; Buntkowsky, G.; Vieth, H.-M.; Pérez-Torrallba, M.; Sanz, D.; Claramunt, R. M.; Elguero, J.; Limbach, H.-H. *J. Am. Chem. Soc.* **2008**, *130*, 8620–8632.
- (15) Lopez, J. M.; Männle, F.; Wawer, I.; Buntkowsky, G.; Limbach, H.-H. *Phys. Chem. Chem. Phys.* **2007**, *9*, 4498–4513.
- (16) Limbach, H.-H.; Lopez, J. M.; Kohen, A. *Philos. Trans. R. Soc. London, Ser. B* **2006**, *361*, 1399–1415.
- (17) Klein, O.; Aguilar-Parrilla, F.; Lopez, J. M.; Jagerovic, N.; Elguero, J.; Limbach, H.-H. *J. Am. Chem. Soc.* **2004**, *126*, 11718–11732.
- (18) Limbach, H.-H.; Klein, O.; Lopez, J. M.; Elguero, J. *Z. Phys. Chem.* **2004**, *218*, 17–49.
- (19) Atwood, J. L.; Barbour, L. J.; Jerga, A. *Science* **2002**, *296*, 2367–2369.
- (20) Prager, M.; Heidemann, A. *Chem. Rev.* **1997**, *97*, 2933–2966.
- (21) Horsewill, A. J. *Prog. Nucl. Magn. Reson. Spectrosc.* **1999**, *35*, 359–389.
- (22) Lang, J.; Deckerová, V.; Czernek, J.; Lhoták, P. *J. Chem. Phys.* **2005**, *122*, 044506/1–044506/11.
- (23) Xin, S. Ph. D. Thesis, Texas Tech. University, Lubbock, TX, 2006.
- (24) Fujimori, H.; Oguni, M. *J. Phys. Chem. Solids* **1993**, *54*, 271–281.
- (25) Matsuo, T.; Oguni, M.; Suga, H.; Seki, S. *Bull. Chem. Soc. Jpn.* **1974**, *47*, 57–66.
- (26) Haida, O.; Matsuo, T.; Suga, H.; Seki, S. *J. Chem. Thermodyn.* **1974**, *6*, 815–825.
- (27) Haida, O.; Suga, H.; Seki, S. *Proc. Jpn. Acad.* **1973**, *49*, 191–195.
- (28) Fujimori, H.; Adachi, Y.; Oguni, M. *Phys. Rev. B* **1992**, *46*, 14501–14504.
- (29) Fujimori, H.; Fujita, H.; Oguni, M. *Bull. Chem. Soc. Jpn.* **1995**, *68*, 447–455.
- (30) Fröhlich, H. *Theory of Dielectrics, Dielectric Constant and Dielectric Loss*; Oxford University Press: Ely House, London, 1958.
- (31) Ichikawa, M. *Acta Crystallogr.* **1978**, *B34*, 2074–2080.
- (32) Benedict, H.; Limbach, H.-H.; Wehlan, M.; Fehlhammer, W.-P.; Golubev, N. S.; Janoschek, R. *J. Am. Chem. Soc.* **1998**, *120*, 2939–2950.
- (33) Sim, G. A.; Robertson, J. M.; Goodwin, T. H. *Acta Crystallogr.* **1955**, *8*, 157–164.
- (34) Bruno, G.; Randaccio, L. *Acta Crystallogr.* **1980**, *B36*, 1711–1712.
- (35) Craven, B. M.; Sabine, T. M. *Acta Crystallogr.* **1966**, *20*, 214–219.
- (36) Alfano, D.; Borrelli, R.; Peluso, A. *J. Phys. Chem. A* **2002**, *106*, 7018–7025.
- (37) Fernandez-Ramos, A.; Smedarchina, Z.; Pichierri, F. *Chem. Phys. Lett.* **2001**, *343*, 627–632.
- (38) Matsuo, T.; Kohno, K.; Inaba, A.; Mochida, T.; Izuoka, A.; Sugawara, T. *J. Chem. Phys.* **1998**, *108*, 9809–9816.
- (39) Kiyonagi, R.; Kimura, H.; Watanabe, M.; Noda, Y.; Mochida, T.; Sugawara, T. *J. Phys. Soc. Jpn.* **2008**, *77*, 064602/1–064602/7.
- (40) Bove, L. E.; Klotz, S.; Paciaroni, A.; Sacchetti, F. *Phys. Rev. Lett.* **2009**, *103*, 165901/1–165901/4.